Model-Independent Z' Limits
from Electron-Electron Collisions

Debajyoti Choudhury, Frank Cuypers

Max-Planck-Institut für Physik, Werner-Heisenberg-Institut, D-80805 München, Germany

Emails: `debchou,cuypers@iws166.mppmu.mpg.de`

Arnd Leike[*]

Sektion Physik der LMU München, Theresienstr. 37, D-80333 München, Germany

Email: `leike@cernvm.cern.ch`

February 7, 2008

Abstract

Model independent constraints on the mass of an extra neutral gauge boson and its couplings to charged leptons are given for the e^-e^- option of a future linear collider. Analytic exclusion limits are derived in the Born approximation. The results are compared with those of the e^+e^- mode. The influence of radiative corrections is discussed.

Electron colliders are usually assumed to be electron-positron colliders. However, this need not necessarily be the case at one of the projected linear colliders such as CLIC, JLC, TESLA, VLEPP, *etc.*. Indeed, a linear collider can also be operated with two colliding electron beams. Such an operation mode has two important advantages: (i) both beams can now be polarized to virtually 100%; (ii) since QCD enters the game only at the two-loop level, e^-e^- collisions provide a very clean environment for detecting slight deviations from the expectations of the electro-weak sector of the standard model. Of the many new possibilities [1, 2, 3, 4], not the least is a search for an extended electro-weak gauge sector.

Model independent constraints on an extra neutral gauge boson Z' have been obtained previously for e^+e^- collisions in Refs [5, 6]. Here, we provide similar bounds for e^-e^- collisions and compare the results with those obtained in e^+e^- collisions. For this we concentrate on a typical linear collider design of the next generation, assuming a center of mass energy $\sqrt{s} = 500$ GeV and an integrated luminosity $\mathcal{L} = 10$ fb^{-1}. These values can anyway be modified trivially. Since very high degrees of longitudinal polarization should be available at future linear colliders, we also assume 100% polarization in the following. The effects of dilution can be easily incorporated, though.

With the introduction of a Z', the Lagrangian for the relevant sector of the theory becomes

$$\mathcal{L} = e \left(A_\mu J_\gamma^\mu + Z_\mu J_Z^\mu + Z'_\mu J_{Z'}^\mu \right), \tag{1}$$

where e is the electric charge and A_μ, Z_μ and Z'_μ represent the photon, the Z-boson and the Z'. The neutral currents are conveniently parametrized as

$$J_i^\mu = \bar{\psi}_e \gamma^\mu \left[R_i P_R + L_i P_L \right] \psi_e \qquad (i = \gamma, Z, Z') , \tag{2}$$

where the left and right projection operators are defined as $P_{R,L} \equiv (1 \pm \gamma_5)/2$. The standard model left- and right-handed couplings L_i and R_i of the vector boson i to electrons are

$$L_\gamma = R_\gamma = -1, \quad L_Z = \tan\theta_W, \quad R_Z = \tan\theta_W - \frac{1}{2\cos\theta_W \sin\theta_W}, \tag{3}$$

where θ_W is the electro-weak mixing angle. The objective is now to obtain constraints on the couplings $L_{Z'}$ and $R_{Z'}$ as a function of $m_{Z'}$.

At the Born level, the scattering $e^-(k_1)e^-(k_2) \rightarrow e^-(p_1)e^-(p_2)$ is described by the exchange of neutral gauge bosons in the $t-$ and/or u–channels, depending on the polarization of the electron beams. As the polarization of the final state electrons is as yet impossible to determine experimentally, the only observable is their angular distribution. We denote the cosine of this angle

$$x = \cos\theta \tag{4}$$

and define

$$x_i = 1 + 2\frac{m_i^2}{s} \qquad (i = \gamma, Z, Z') . \tag{5}$$

1

Neglecting the electron mass and the widths of the gauge bosons, we have for the three possible combinations of beam polarizations

$$
\begin{aligned}
\frac{d\sigma^{LL}}{dx} &= \frac{16\pi\alpha^2}{s} \sum_{i,j=\gamma,Z,Z'} L_i^2 L_j^2 \left[\frac{x_i x_j}{(x_i^2 - x^2)(x_j^2 - x^2)} \right] \\
\frac{d\sigma^{RR}}{dx} &= \frac{16\pi\alpha^2}{s} \sum_{i,j=\gamma,Z,Z'} R_i^2 R_j^2 \left[\frac{x_i x_j}{(x_i^2 - x^2)(x_j^2 - x^2)} \right] \\
\frac{d\sigma^{LR}}{dx} &= \frac{\pi\alpha^2}{s} \sum_{i,j=\gamma,Z,Z'} L_i R_i L_j R_j \left[\frac{(1+x)^2}{(x_i - x)(x_j - x)} + \frac{(1-x)^2}{(x_i + x)(x_j + x)} \right] \\
\frac{d\sigma^{\text{Unp.}}}{dx} &= \frac{1}{4} \left(\frac{d\sigma^{LL}}{dx} + \frac{d\sigma^{RR}}{dx} + 2\frac{d\sigma^{LR}}{dx} \right) \;,
\end{aligned}
\tag{6}
$$

where $\alpha = e^2/4\pi$ is the fine structure constant. Note that since the polarization of the final state electrons cannot be measured, one has to sum over their polarizations. This is why in the LR case the angular distribution remains symmetric.

As expected for Møller scattering, the distribution becomes singular for $|x| \to 1$. Had we retained the electron mass, it would have regulated this collinear singularity arising from diagrams with photon exchange. This contribution is nonetheless eliminated naturally by the experimental acceptance cut on the angle of the emergent electron, $|x| < x_+$.

Before embarking on a more detailed analysis, let us estimate the resolving power of this reaction in the limit where $m_{Z'} \gg \sqrt{s} \gg m_Z$, hence neglecting terms of $O(M_Z^2/s)$ and $O(s/M_{Z'}^2)$. The differences between the cross sections expected in the presence and the absence of a Z' become then

$$
\Delta\sigma_{LL} = L'^2 \quad \frac{16\pi\alpha^2}{s} \quad \frac{1}{\cos^2\theta_W} \quad \ln\frac{1+x_+}{1-x_+}
\tag{7}
$$

$$
\Delta\sigma_{RR} = R'^2 \quad \frac{16\pi\alpha^2}{s} \frac{1}{4\sin^2\theta_W \cos^2\theta_W} \ln\frac{1+x_+}{1-x_+}
\tag{8}
$$

$$
\Delta\sigma_{LR} = L'R' \quad \frac{4\pi\alpha^2}{s} \quad \frac{1}{\cos^2\theta_W} \quad \left(\ln\frac{1+x_+}{1-x_+} - \frac{3}{2}x_+ \right) \;,
\tag{9}
$$

where we defined the reduced left and right Z' couplings

$$
L' = \frac{\sqrt{s}}{m_{Z'}} L_{Z'}
\tag{10}
$$

$$
R' = \frac{\sqrt{s}}{m_{Z'}} R_{Z'} \;.
\tag{11}
$$

Demanding that the difference in the number of events is sufficiently significant, leads to simple bounds on these reduced coupling. Several features of the analysis are clear:

- The dependence on the Z' mass has been absorbed into the definition (10,11) of the reduced couplings.

2

- The LL mode, with both beams left–polarized, is sensitive only to the coupling L', and similarly for right polarization. There is thus no correlation between these two complementary measurements, which yield straight vertical and horizontal bands for the detectability limits in the (L', R') plane.

- In contrast, the experiment with LR beams yields highly correlated information on the L' and R' parameters. The curves delimiting the detectability region are now hyperbolas.

- In the limit where $\sin^2 \theta_W = 1/4$ the LL and RR modes have the same resolving power. In practice, the RR mode yields only a minute improvement. The LR mode, however, is much less sensitive.

All these features remain accurate in the more precise analysis which is to follow now.

To take advantage of the angular information contained in Eqs (6), we consider a moderate number N of bins in $x = \cos\theta$ and compare the observed number of events n_i in each with the standard model expectations n_i^{SM}. Denoting the fraction of events in each bin by

$$X_i = \frac{n_i}{n} \tag{12}$$

where $n = \sum_{i=1}^{N} n_i$, a χ^2 test for the deviation can be devised as

$$\chi^2 = \sum_{i=1}^{N} \left(\frac{X_i - X_i^{SM}}{\Delta X_i} \right)^2 . \tag{13}$$

The corresponding statistical error in the bin i is given by

$$\Delta X_i^2 = \frac{n_i}{n^2} \left(1 - \frac{n_i}{n} \right) . \tag{14}$$

The second term in Eq. (14) originates from the correlation between the number of events in one bin and the total number of events. The advantage of using the relative numbers of events $X_i = n_i/n$ resides in the fact that the systematic error due to uncertainties in the luminosity measurements drops out.

Armed with the above expressions, we can now examine the observabilty of the reduced Z' couplings (10,11). For concreteness we assume a center of mass energy of 500 GeV and an integrated luminosity of $10 \, \text{fb}^{-1}$. We impose the symmetrical angular cut

$$|x| < x_+ = 0.985 \tag{15}$$

and divide this range into $N = 10$ equal size bins. Since we deal here with one-sided bounds the exclusion contours at 95% confidence level in the (L', R') plane are identified by demanding $\chi^2 > 4.61$ in Eq. (13). These contours are depicted for $m_{Z'} = 2$ TeV in Fig. 1 for LL, RR and LR beam polarizations. These exclusion regions are indeed bounded by straight lines and hyperbolas, as expected from the crude analysis based on Eqs (7-9).

Obviously, unpolarized beams are less sentive. The combined fit $\chi^2 = \chi^2_{LL} + \chi^2_{RR} + \chi^2_{LR}$ does not yield very much additional information, since the two most sensitive measurements (LL and RR) already provide uncorrelated results.

While the results in Fig 1 are strictly speaking valid only for the particular value 2 TeV of the Z' mass, the generic features prevail for other masses too. Indeed, the limits of detectability of L' and R' in the LL and RR experiments, depend very little on the details of the analysis. This can be infered from the plots in Figs 2, 3 and 4, where the smallest detectable value of R' with 95% confidence (since the value taken by L' is irrelevant, this is only a one-parameter fit, hence $\chi^2 = 2.71$), is plotted respectively as a function of the cut x_+, the number of bins N, and the mass $m_{Z'}$ of the Z'. The reduced coupling L' yields nearly undistinguishable results (which would actually be identical for $\sin^2\theta_W = 1/4$).

In Fig. 4 we have also plotted the discovery limits which can be achieved by a LR asymmetry measurement[1] in e^+e^- collisions, under the same conditions. Clearly, on the Z' peak (here at 500 GeV) e^+e^- collisions provide almost unlimited precision. However, if the Z' mass exceeds the center of mass energy by as little as 20%, the e^-e^- mode with both beams polarized provides already more accurate bounds. Asymptotically, roughly a factor of 1.6 can be achieved.

Finally, we want to comment on radiative corrections. The considered reaction has no resonating behaviour with the center of mass energy $\sqrt{s}$. However, the cross section has a very singular angular dependence keeping most of the outgoing electrons at very small angles in the beam pipe. The radiation of hard photons could kick an electron from the beam pipe into the detector. Nevertheless, the corresponding hard photon can of course be vetoed. The radiation of collinear hard photons from the initial state reduces the effective energy of the colliding electrons giving a lower sensitivity to a Z'. However, such events can also be removed by demanding that the energy of the scattered electrons be close to the beam energy. To summarize, radiative corrections are not expected to induce sizable changes to our model independent Z' limits obtained at the Born level.

To conclude, we have demonstrated the excellent potential of e^-e^- collisions in constraining Z' physics. Model independent limits have been derived, which are much more stringent than those that could be obtained in e^+e^- collisions.

Acknowledgement

---

[1] This turns out to be the most sensitive experiment of Ref. [5] to the variable R'

References

[1] P.H. Frampton and D. Ng, *Phys. Rev.* **D 45** (1992) 4240.

[2] F. Cuypers, G.J. van Oldenborgh and R. Rückl, *Nucl. Phys.* **B 409** (1992) 128.

[3] C.A. Heusch and P. Minkowski, CERN preprint CERN-TH-6606-92, May 1993.

[4] D. Choudhury and F. Cuypers, MPI preprint MPI-Ph/94-24.

[5] A. Leike, DESY 93-154, to appear in Z. Phys. **C**.

[6] F. del Aguila, UG-FT-35/94.

[7] A. Djouadi, A. Leike, T. Riemann, D. Schaile, C. Verzegnassi, Proc. of the "Workshop on Physics and Experiments with Linear Colliders", Sept. 1991, Saariselkä, Finland, ed. R. Orava, Vol. II, p. 515;
A. Djouadi, A. Leike, T. Riemann, D. Schaile, C. Verzegnassi, Z. Phys. **C56** (1992) 289.

Figure Captions

Fig. 1 Contours of Eq. (13) for $\chi^2 = 4.61$ in the plane of the reduced Z' couplings (L', R') (10,11), for different combinations of beam polarizations. The combined fit of the LL, RR and LR polarizations is also shown.

Fig. 2 Dependence of the smallest observable value of the reduced coupling R' (11) with 95% confidence, as a function of the angular cut (15).

Fig. 3 Dependence of the smallest observable value of the reduced coupling R' (11) with 95% confidence, as a function of the number of bins in Eq. (13).

Fig. 4 Dependence of the smallest observable value of the reduced coupling R' (11) with 95% confidence, as a function of the mass of the Z'.
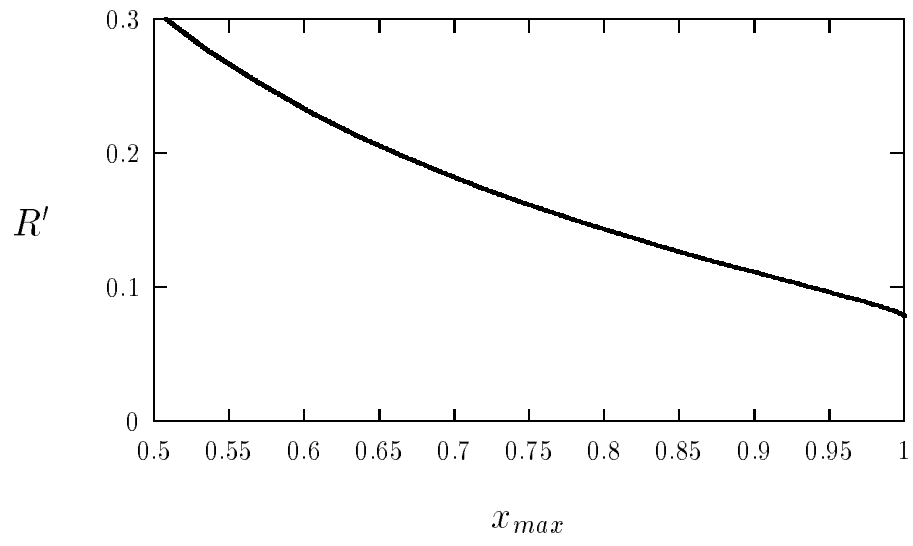
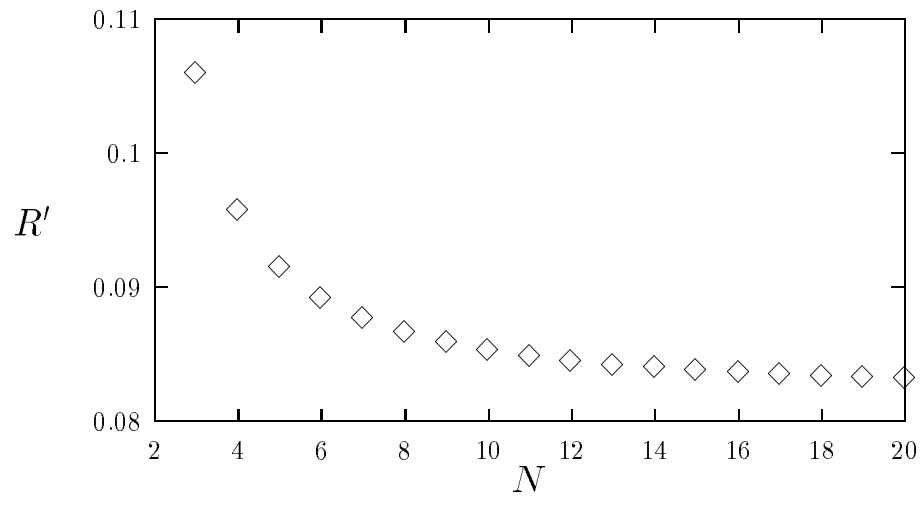This figure "fig1-1.png" is available in "png" format from:

http://arXiv.org/ps/hep-ph/9404362v1
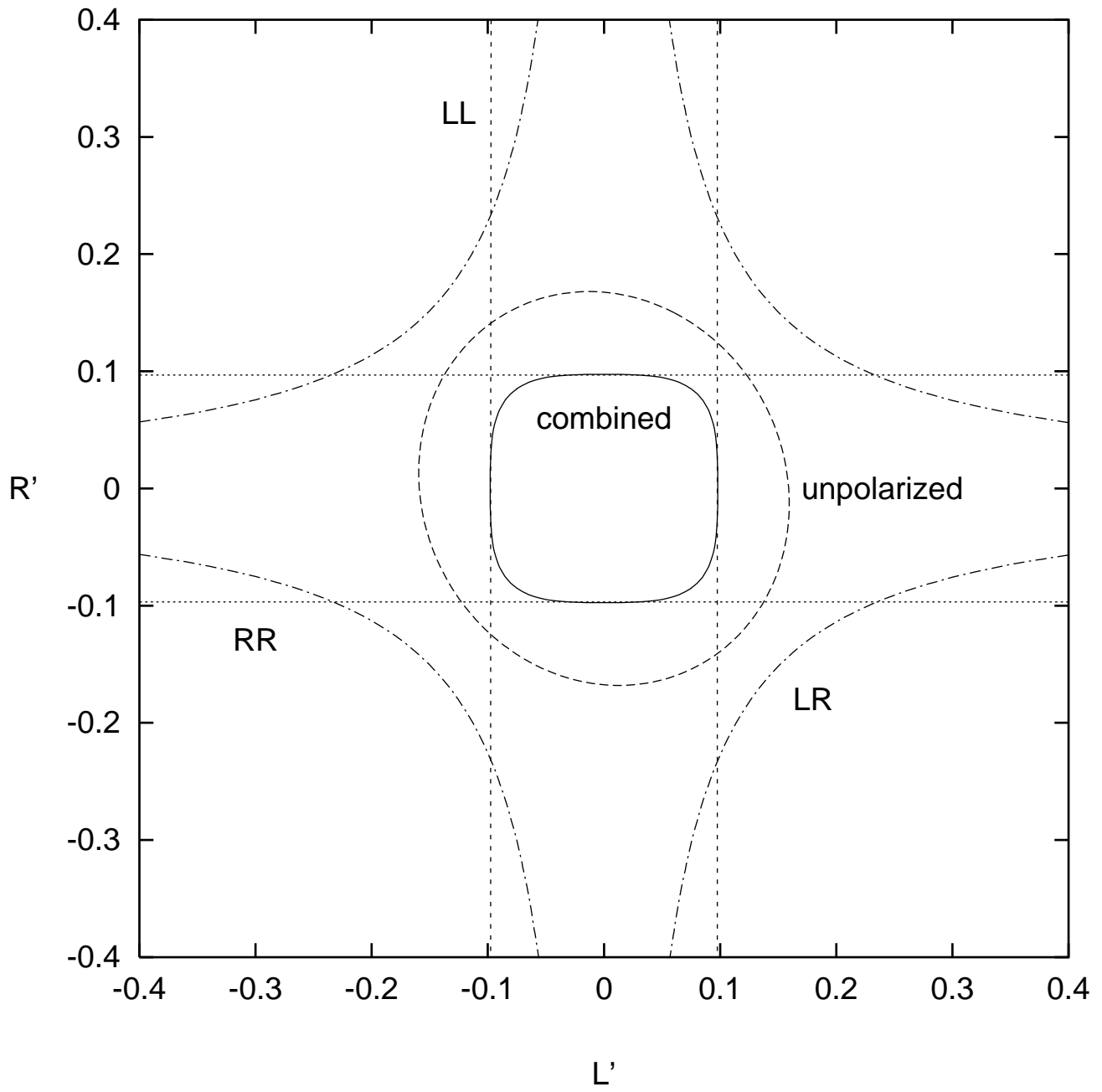
This figure "fig1-2.png" is available in "png" format from:

http://arXiv.org/ps/hep-ph/9404362v1

This figure "fig1-3.png" is available in "png" format from:

http://arXiv.org/ps/hep-ph/9404362v1

This figure "fig1-4.png" is available in "png" format from:

http://arXiv.org/ps/hep-ph/9404362v1